The Effect of Substitution Position on Intramolecular Charge-Transfer in Carbazole-Pyridine Derivatives

DOI: 10.23977/mpcr.2025.050109 ISSN 2616-1702 Vol. 5 Num. 1

Fangyi Chen, Mingjie Li, Xiunan Xu

Chongqing College of Electronic Engineering, No.76 University Town East Road, Shapingba District, Chongqing, 401331, China

Keywords: Intramolecular Charge Transfer (ICT); Substitution Position; Photoluminescent Properties; Density Functional Theory (DFT)

Abstract: This study focused on a series of carbazole-pyridine derivatives with symmetric D-A-D structures, where pyridine rings serve as the center and carbazoles are distributed on both sides of the pyridine rings, to investigate atomic-level insights into how atomic charge and distance affect ICT. This study demonstrates that substitution position regulates ICT properties by influencing molecular conformation and electron transfer efficiency, laying a theoretical foundation for the development of high-performance D-A type organic small molecules.

1. Introduction

Organic optoelectronic materials have garnered significant attention in recent decades due to their advantages of flexibility, low cost, and easy processing, with Donor-Acceptor (D-A) type organic small molecules being one of the most important research directions[1]. The core characteristic of D-A molecules is Intramolecular Charge Transfer (ICT), where electrons transfer from electron-donating groups to electron-accepting groups upon photoexcitation, which directly determines their optical and electrical properties [2]. Factors such as the type, number, and relative position of donors and acceptors can modulate ICT behavior. Among these, the relative position of donors and acceptors is a key structural parameter, as it affects molecular conformation, π -conjugation degree, and electron distribution—all of which are closely related to ICT efficiency[3].

Carbazole is a widely used electron donor in organic optoelectronic materials due to its good electron-donating ability, high thermal stability, and adjustable molecular structure[4]. Pyridine, with its electron-deficient heterocyclic structure, serves as an excellent electron acceptor [5]. Carbazole-pyridine derivatives, as typical D-A systems, have shown potential applications in organic light-emitting diodes and fluorescent probes. However, most previous studies on carbazole-pyridine derivatives have focused on modifying the type of donors/acceptors or adjusting the length of π -conjugated bridges, while the effect of substitution position of carbazole on the pyridine ring (a subtle but critical structural factor) on ICT properties remains insufficiently explored[6].

To address this gap, this study designed and synthesized three carbazole-pyridine derivatives with symmetric D-A-D structures (Figure 1), where carbazoles are substituted at different positions

on the pyridine ring. The photoluminescent properties (absorption spectra, emission spectra, fluorescence quantum efficiency, and Stokes shift) of these compounds in solvents of varying polarity were systematically characterized to analyze their ICT behaviors. Additionally, DFT and TD-DFT calculations were employed to optimize molecular geometric structures, calculate electron transition energies, and simulate electron density changes, revealing the intrinsic mechanism by which substitution position regulates ICT properties. This work not only enriches the understanding of structure-activity relationships in D-A type organic molecules but also provides a theoretical basis for the rational design of high-performance organic optoelectronic materials.

Figure 1 Molecular structures of series carbazole-pyridine compounds

2. Experimental and computational details

2.1 Synthesis of Carbazole-Pyridine Derivatives

The target compounds were synthesized via Suzuki coupling reaction.(Figure 2) A typical synthesis procedure for 26-CzPy is as follows: Under an argon atmosphere, 2,6-dibromopyridine (1.0 mmol), carbazole-2-boronic acid (2.2 mmol), Pd(pph₃)₄ (0.05 mmol), and K₂CO₃ (3.0 mmol) were added to a round-bottom flask containing a mixed solvent of dioxane and water (4:1, v/v). The reaction mixture was refluxed at 100 °C for 24 h. After cooling to room temperature, the mixture was extracted with dichloromethane, and the organic layer was dried over anhydrous MgSO₄. The crude product was purified by column chromatography on silica gel using petroleum ether/ethyl acetate (5:1, v/v) as the eluent, yielding a white solid (26-CzPy, yield: ~75%). The synthesis procedures for 35-CzPy (using 3,5-dibromopyridine) and 24-CzPy (using 2,4-dibromopyridine) were similar to that of 26-CzPy, with yields of ~72% and ~70%, respectively. The structures of the compounds were confirmed by H NMR, ¹C NMR, and high-resolution mass spectrometry (HRMS).

All chemical reagents were purchased from commercial sources (Sigma-Aldrich, Aladdin) and used without further purification unless otherwise stated.

$$X^5$$
 X^4
 X^5
 X^5
 X^6
 X^7
 X^8
 X^8

26-CzPy: $X^3=X^4=X^5=Y^3=Y^4=Y^5=H$, $X^2=X^6=F$, $Y^2=Y^6=Cz$ 35-CzPy: $X^2=X^4=X^6=Y^2=Y^4=Y^6=H$, $X^3=X^5=F$, $Y^3=Y^5=Cz$ 24-CzPy: $X^3=X^5=X^6=Y^3=Y^5=Y^6=H$, $X^2=X^4=F$. $Y^2=Y^4=Cz$

Figure 2 Synthesis of a series of carbazole-pyridine compounds

2.2 Experimental and Computational details

UV-visible absorption spectra were recorded on a Shimadzu UV-2600 spectrophotometer, and fluorescence emission spectra were measured using a Hitachi F-7100 fluorescence spectrophotometer. To ensure the compounds existed in a monomolecular state, the concentrations of 24-czpy and 26-czpy solutions were adjusted to 1×10^{-5} M, and the concentration of 35-czpy solution was 6×10^{-6} M.

Fluorescence quantum efficiency (Φ) was determined using the relative method, with quinine sulfate in 0.5 M H₂SO₄ (Φ = 0.54) as the reference standard. The quantum efficiency was calculated using the equation: Φ _sample = Φ _ref × (I_sample / I_ref) × (A_ref / A_sample) × (n_sample² / n_ref 3), where I is the integrated fluorescence intensity, A is the absorbance at the excitation wavelength, and n is the refractive index of the solvent.

All theoretical calculations were performed using the Gaussian 16 software package. Electron density difference maps were analyzed using Multiwfn software and molecular structures were visualized with VMD software [7-11].

3. Results and Discussion

3.1 Avoidance strategies

The UV-visible absorption spectra and fluorescence emission spectra of 26-CzPy, 35-CzPy, and 24-CzPy in solvents of different polarities are shown in Figure 3.

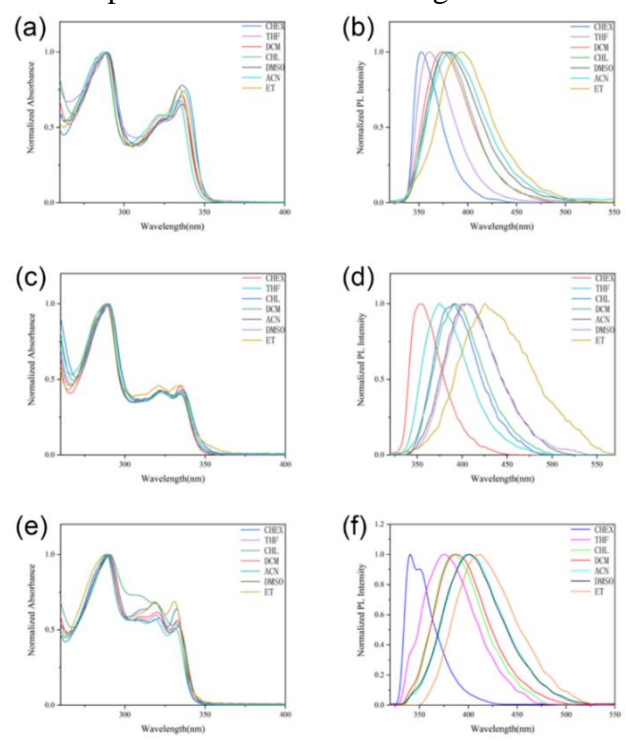


Figure 3 Normalized UV-visible absorption spectra of three molecules

3.1.1 Absorption Spectra

All three compounds exhibited three distinct absorption peaks around 290 nm, 325 nm, and 335 nm in various solvents, which can be attributed to π – π * transitions (as confirmed by theoretical calculations). When solvent polarity increased from non-polar cyclohexane to polar acetonitrile, the

maximum absorption peaks of the three compounds only showed a slight redshift (~3 nm). This small redshift indicates that the electronic structure and properties of the Franck-Condon (FC) excited state of the compounds change minimally compared to the ground state, suggesting that the ground-state and FC excited-state structures are relatively similar.

3.1.2 Emission Spectra

In contrast to the absorption spectra, the emission spectra of the compounds showed significant solvent dependence. For 26-CzPy, the maximum emission peak was 353 nm in cyclohexane, 377 nm in chloroform, 361 nm in THF, 375 nm in DCM, 393 nm in ethanol, 383 nm in acetonitrile, and 379 nm in DMSO. When solvent polarity increased from cyclohexane to acetonitrile, the maximum emission peak of 26-czpy redshifted by approximately 30 nm. For 35-czpy and 24-czpy, the redshifts of the maximum emission peaks under the same solvent polarity change were 53 nm and 61 nm, respectively (Table 1). This significant redshift of emission peaks with increasing solvent polarity confirms that the excited states of the compounds undergo ICT. The ICT process is driven by the relaxation of the FC excited state and solvent-induced charge redistribution: in polar solvents, the solvent molecules align with the dipole moment of the excited state, stabilizing the ICT state and reducing its energy, thereby causing a redshift in the emission spectrum.

Notably, 24-Czpy exhibited a shoulder peak at 350.5 nm in cyclohexane, which disappeared as solvent polarity increased. This phenomenon is attributed to vibrational energy levels of the molecule in low-polarity solvents: in non-polar solvents, the molecule has more vibrational modes, leading to the appearance of shoulder peaks; in polar solvents, strong solvent-molecule interactions suppress molecular vibrations, resulting in the disappearance of shoulder peaks.

3.1.3 Fluorescence Quantum Efficiency

The fluorescence quantum efficiencies of the three compounds in different solvents are listed in Table 1. For 26-CzPy, the quantum efficiency was 0.36 in non-polar cyclohexane and decreased to 0.25 in polar acetonitrile. 35-CzPy had quantum efficiencies of 0.13 in cyclohexane and 0.21 in THF (low polarity), which further decreased to 0.11 in acetonitrile and 0.05 in ethanol (high polarity). 24-CzPy showed a quantum efficiency of 0.27 in cyclohexane and 0.15–0.21 in high-polarity solvents (ethanol and acetonitrile).

The decrease in fluorescence quantum efficiency with increasing solvent polarity is a typical characteristic of ICT molecules. In polar solvents, the ICT state of the molecule interacts strongly with solvent molecules, promoting non-radiative relaxation processes (e.g., internal conversion and intersystem crossing), which increases the non-radiative decay rate and thus reduces the quantum efficiency. Additionally, molecular conformation (torsion angle between carbazole and pyridine rings) also affects quantum efficiency. As shown in Table 1, the torsion angles between the benzene rings (on carbazole) and the central pyridine ring were ~40 ° for 26-CzPy, ~54 ° for 35-CzPy, and ~40 %48 ° for 24-CzPy in the ground state. The larger the torsion angle, the lower the quantum efficiency: 35-CzPy (largest torsion angle) had the lowest quantum efficiency, while 26-CzPy (smallest torsion angle) had the highest. This is because a smaller torsion angle enhances the planarity of the molecule, reducing the non-radiative decay caused by molecular vibrations and rotations, thereby improving the fluorescence quantum efficiency.

3.1.4 Stokes Shift

Stokes shift (Δv_st) was calculated using the maximum values of absorption and emission spectra, and the results are shown in Table 1 and Figure 4. The Stokes shifts of 26-CzPy, 35-CzPy, and 24-czpy in solvents ranging from cyclohexane (polarity parameter $\Delta f = 0.007$) to ethanol ($\Delta f = 0.007$) to ethanol ($\Delta f = 0.007$) to expect the solution of the stokes shifts of 26-CzPy, 35-CzPy, and 24-czpy in solvents ranging from cyclohexane (polarity parameter $\Delta f = 0.007$) to ethanol ($\Delta f = 0.007$) to expect the solution of the solution of the stokes shifts of 26-CzPy, 35-CzPy, and 24-czpy in solvents ranging from cyclohexane (polarity parameter $\Delta f = 0.007$) to ethanol ($\Delta f = 0.007$) to expect the solution of the solution of the stokes shifts of 26-CzPy.

0.290) were 6100–9400 cm⁻¹, 6100–11000 cm⁻¹, and 5200–11000 cm⁻¹, respectively. All three compounds showed an increase in Stokes shift with increasing solvent polarity, which confirms that the ICT excited state is stabilized in polar solvents.

The Lippert-Mataga equation was used to calculate the change in dipole moment ($\Delta \mu = \mu CT - \mu$ g) from the ground state to the ICT excited state[19,20]:

$$\Delta v \text{ st} = (2/4\pi\epsilon_0 hc\alpha^3) \times (\mu \text{ CT} - \mu \text{ g})^2 \times \Delta f(\epsilon, \eta) + C$$

Where Δv _st is the Stokes shift, h is Planck's constant, c is the speed of light, ϵ_0 is the vacuum permittivity, μ _g is the ground-state dipole moment, μ _CT is the ICT excited-state dipole moment, $\Delta f(\epsilon, \eta)$ is the solvent polarity parameter ($\Delta f = (\epsilon - 1)/(2\epsilon + 1) - (\eta^2 - 1)/(2\eta^2 + 1)$, where ϵ is the solvent dielectric constant and η is the refractive index), α is the solvent cavity radius, and C is a constant.

The solvent cavity radii (α) of 26-CzPy, 35-CzPy, and 24-CzPy, calculated using DFT with the B3LYP/6-31G(d,p) basis set, were 5.34 Å, 5.66 Å, and 5.42 Å, respectively. As shown in Figure 4, the Stokes shifts of the three compounds exhibited a good linear correlation with the solvent polarity parameter Δf , but the slopes of the fitting lines were different, indicating differences in their dipole moment changes. The calculated $\Delta \mu$ values were 14.0 D for 26-CzPy, 19.6 D for 35-CzPy, and 19.6 D for 24-CzPy. The order of $\Delta \mu$ (24-CzPy \approx 35-CzPy > 26-CzPy) is consistent with the redshift trend of the emission peaks, confirming that the ICT intensity is positively correlated with the change in dipole moment.

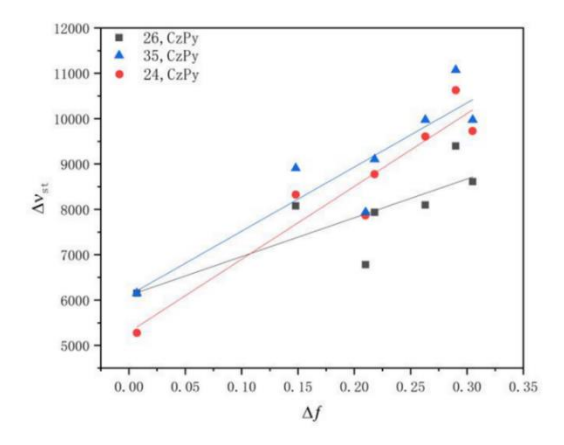


Figure 4 Relationship between stokes displacement and solvent polarizability of 26-CzPy, 35-CzPy and 24-CzPy molecules in different solvents

3.2 Theoretical study

3.2.1 Molecular geometry

The ground-state (S₀) and excited-state (S₁) geometric structures of 26-CzPy, 35-CzPy, and 24-CzPy were optimized using DFT/B3LYP/6-31G(d,p), and the key structural parameters (bond lengths and torsion angles) are summarized in Figures 5.

In the ground state, all three compounds adopted a V-shaped structure, with the carbazole groups and pyridine ring showing a certain degree of torsion. For 26-czpy, the torsion angles between the two carbazole groups (Cz1 and Cz2) and the pyridine ring (Py) were both ~40°, and the bond lengths of the C-N bonds (11 and 12) connecting carbazole and pyridine were both 1.41 Å. For 35-CzPy, the torsion angles between Cz1/Cz2 and Py were ~54°, and the C-N bond lengths were 1.41 Å. For 24-CzPy, the torsion angles between Cz1/Cz2 and Py were ~40° and ~49°, respectively,

with C-N bond lengths of 1.41 Å.

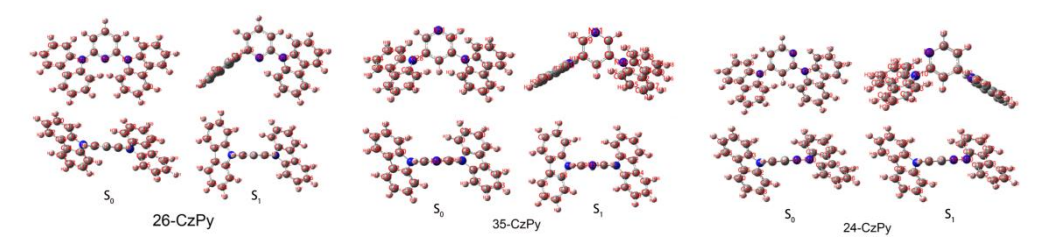


Figure 5 Geometrically optimized structure of 26-CzPy, 35-CzPy and 24-CzPy

Upon excitation to the S_1 state, the torsion angles and C-N bond lengths of all three compounds increased. For 26-CzPy, the torsion angles of Cz1-Py and Cz2-Py increased to ~53 ° and ~86 °, and the C-N bond lengths increased to 1.47 Å and 1.43 Å. For 35-CzPy, the torsion angles increased to ~96 ° and ~62 °, and the C-N bond lengths increased to 1.45 Å and 1.43 Å. For 24-CzPy, the torsion angles increased to ~74 ° and ~83 °, and the C-N bond lengths increased to 1.47 Å and 1.42 Å. These changes in geometric parameters indicate that substitution position affects molecular conformation: different substitution positions lead to differences in the steric hindrance between carbazole and pyridine groups, resulting in different torsion angles. The increase in torsion angles and C-N bond lengths in the excited state is due to the ICT process: electron transfer from carbazole (donor) to pyridine (acceptor) changes the electron density of the C-N bond, weakening the bond strength and increasing the bond length, while the increased torsion angle reduces the overlap between the π orbitals of carbazole and pyridine, thereby adjusting the ICT efficiency.

3.2.2 Electronic Transitions and Frontier Molecular Orbitals

The excitation energies and oscillator strengths of the five lowest excited states (S_1 – S_5) of the compounds in cyclohexane and acetonitrile were calculated using TD-DFT, and the results are shown in Table 1. For 26-CzPy and 24-CzPy, the highest allowed transition was $S_0 \rightarrow S_1$, with excitation energies of 3.72 ev and 3.73 ev, and oscillator strengths of 0.32 and 0.27, respectively. For 35-czpy, the highest allowed transition was $S_0 \rightarrow S_3$, with an excitation energy of 3.94 eV and an oscillator strength of 0.21. The oscillator strength reflects the probability of electronic transitions: a higher oscillator strength indicates a more probable transition.

Table 1 B3LYP/ 6-31g (d, p) method was used to calculate the excitation energy (eV) and vibrator intensity (f) of each molecule in the five lowest excited states in the solution model.

	26-CzPy		35-CzPy		24-CzPy	
	Calculated excitation energy (eV)					
	CHEX	CAN	CHEX	ACN	CHEX	ACN
S1	3.72	3.78	3.64	3.68	3.73	3.77
S2	3.99	4.04	3.74	3.77	3.90	3.92
S3	4.07	4.07	3.94	3.98	4.07	4.09
S4	4.08	4.08	3.98	4.01	4.10	4.10
S5	4.11	4.17	4.06	4.06	4.13	4.18
	oscillator strengths					
S1	0.32	0.31	0.12	0.11	0.24	0.27
S2	0.02	0.03	0	0	0.17	0.11
S3	0.08	0.02	0.21	0.20	0.19	0.09
S4	0.19	0.06	0.04	0.03	0.03	0.17
S5	0.04	0.08	0.06	0.03	0.01	0.11

The relationship between fluorescence quantum efficiency and oscillator strength of the first

excited state (S_1) was further analyzed. In cyclohexane, 26-CzPy had a quantum efficiency of 0.36 and an $S_0 \rightarrow S_1$ oscillator strength of 0.32; 35-CzPy had a quantum efficiency of 0.13 and an $S_0 \rightarrow S_1$ oscillator strength of 0.12; 24-CzPy had a quantum efficiency of 0.27 and an $S_0 \rightarrow S_1$ oscillator strength of 0.24. This indicates that the fluorescence quantum efficiency increases with the oscillator strength of the S_1 state: a higher oscillator strength enhances the radiative transition probability from the S_1 state to the ground state (S_0), thereby increasing the quantum efficiency.

The frontier molecular orbitals (HOMO: Highest Occupied Molecular Orbital; LUMO: Lowest Unoccupied Molecular Orbital) of the compounds were analyzed to understand the electron transfer direction during ICT(figure 6). For 26-CzPy, the HOMO orbital electron density is distributed on the carbazole groups, while the LUMO orbital electron density is localized on the pyridine ring. The $S_0 \rightarrow S_1$ transition is mainly a HOMO \rightarrow LUMO transition (contribution: 98%), indicating that electrons transfer from the two carbazole groups to the central pyridine ring during ICT. For 35-czpy, the $S_0 \rightarrow S_3$ transition (main transition) is a H-1 \rightarrow L+1 transition (contribution: 98%), with the H-1 orbital electron density on the carbazole groups and the L+1 orbital electron density on the pyridine ring, also showing electron transfer from carbazole to pyridine. For 24-CzPy, the $S_0 \rightarrow S_1$ transition is a HOMO \rightarrow LUMO transition (contribution: 90%), where the HOMO orbital electron density is on one carbazole group and the LUMO orbital electron density is on the pyridine ring, indicating one-sided electron transfer from carbazole to pyridine. These results confirm that carbazole acts as the electron donor and pyridine as the electron acceptor in the compounds, and the substitution position affects the electron transfer path (bilateral vs. one-sided transfer), thereby regulating ICT intensity.

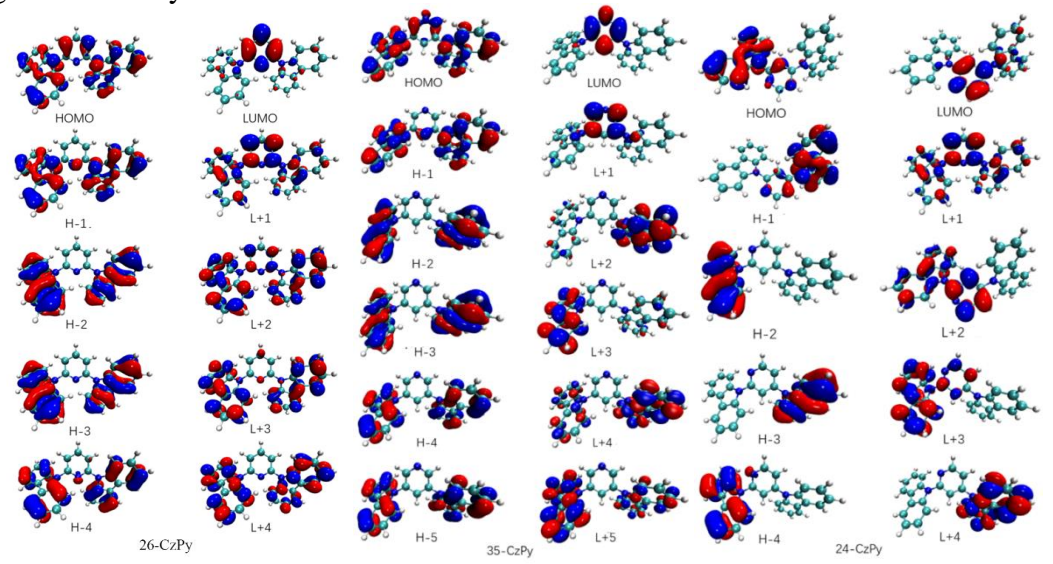


Figure 6 Composition of the main frontier molecular orbitals of 26-CzPy, 35-CzPy and 24-CzPy (B3LYP/6-31G(d, p) method)

3.2.3 EIntramolecular charge transfer

Electron density difference maps (EDDMs) were used to visualize the electron density changes from the ground state to the excited state (Figure 7). In the EDDMs, yellow regions represent increased electron density, and cyan regions represent decreased electron density. For 26-CzPy, the electron density of the carbazole groups decreases (cyan) and that of the pyridine ring increases (yellow) in the S₁ state, indicating electron transfer from both carbazole groups to the pyridine ring. For 35-CzPy, the electron density of the carbazole groups decreases and that of the pyridine ring increases in the S₃ state, also showing bilateral electron transfer. For 24-CzPy, only one carbazole

group shows decreased electron density, while the other carbazole group has no significant electron density change, and the pyridine ring shows increased electron density, confirming one-sided electron transfer.

The atomic charge changes from the ground state to the excited state were quantified using the Atom Dipole Corrected Hirshfeld (ADCH) method. For 26-CzPy, the charge changes of Cz1 and Cz2 (donors) were -0.145 |e| each, indicating that each carbazole group donates 0.145 |e|. For 35-CzPy, the charge changes of Cz1 and Cz2 were -0.173 |e| each. For 24-CzPy, the charge change of Cz1 was -0.290 |e|, while Cz2 had no charge change (0 |e|). The total charge transferred to the pyridine ring was 0.277 |e| (26-CzPy), 0.326 |e| (35-CzPy), and 0.290 |e| (24-CzPy), which is consistent with the dipole moment change results. Additionally, the charge transfer distance (from the carbazole charge center to key atoms on the pyridine ring) was analyzed. The distances were similar among the three compounds (3.1–5.8 Å), indicating that substitution position has a minor effect on charge transfer distance but a significant effect on charge transfer amount—thus regulating ICT intensity.

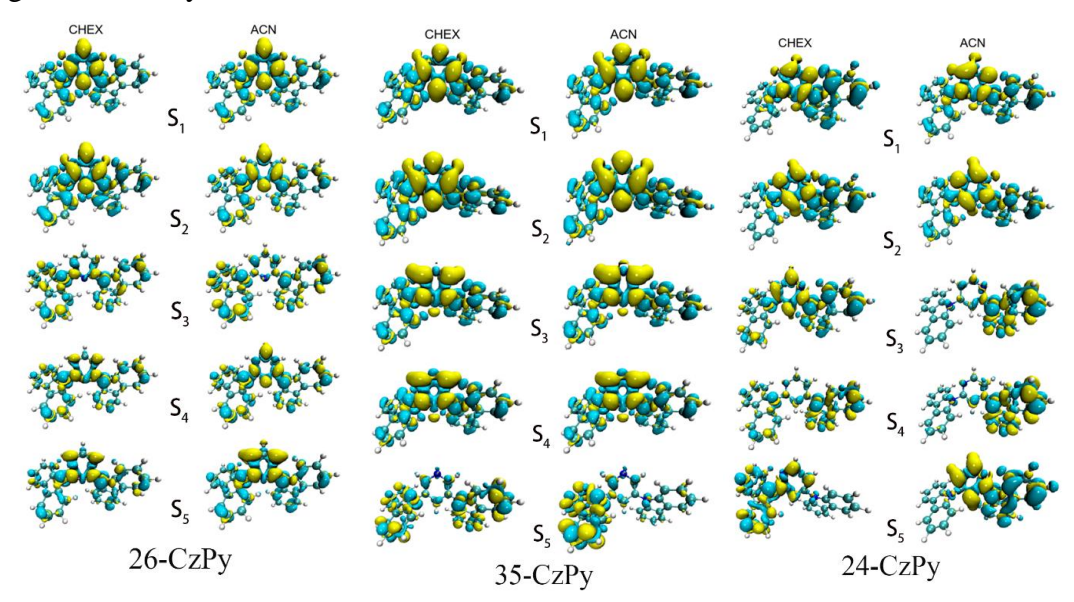


Figure 7 Electron density difference between ground and excited states of 26-CzPy, 35-CzPy and 24-CzPy in different polar solvent models.

4. Conclusions

This study systematically investigated the effect of carbazole substitution position on the intramolecular charge transfer (ICT) properties of carbazole-pyridine derivatives through experimental characterization and theoretical simulations. This work demonstrates that substitution position is a critical parameter for regulating the ICT properties of D-A type organic small molecules. By adjusting the substitution position, the ICT intensity and fluorescence quantum efficiency can be effectively tuned, providing a new strategy for the design of high-performance organic optoelectronic materials.

Acknowledgments

This work was supported by Scientificand Technological Research Program of Chongqing Municipal Education Commission (Grant No.KJQN202203118)

References

- [1] Han, X.; Hu, F.; Chi, W.; Ma, X.; Liu, S. H.; Liu, X.; Yin, J., Unusual intermolecular charge transfer enables supramolecular fluorescent viscosity sensors [J]. Sensors and Actuators B: Chemical 2018, 277, 55-61.
- [2] Amadei, A.; D'Abramo, M.; Nola, A. D.; Arcadi, A.; Cerichelli, G.; Aschi, M., Theoretical study of intramolecular charge transfer in π -conjugated oligomers [J]. Chemical Physics Letters 2007, 434 (4-6), 194-199.
- [3] Cui, Y.; Li, P.; Song, C.; Zhang, H.., Terminal Modulation of D- π -A Small Molecule for Organic Photovoltaic Materials: A Theoretical Molecular Design, The Journal of Physical Chemistry C [J]. 2016, 120 (51), 28939-28950.
- [4] Feezell, D.; Nakamura, S., Invention, development, and status of the blue light-emitting diode, the enabler of solid-state lighting [J]. Comptes Rendus Physique 2018, 19 (3), 113-133.
- [5] Brancato, G.; Zerbetto, F., On the distribution of local molecular symmetry in crystals [J]. Journal of Physical Chemistry A 2000, 104 (48), 11439-11442.
- [6] Zhao, C.; Zhao, Y.; Lin, J., Optoelectronic Materials of Organoboron pi-Conjugated Systems [J]. Progress in Chemistry 2009, 21 (12), 2605-2612.
- [7] Frisch M J, Trucks G W, Schlegel H B, Scuseria G E, Robb M A, Cheeseman J R, Scalmani G, Barone V, Petersson G A, Nakatsuji H, Li X, Caricato M, Marenich A, Bloino J, Janesko B G, Gomperts R, Mennucci B, Hratchian H P, Ortiz J V, Izmaylov A F, Sonnenberg J L, Williams-Young D, Ding F, Lipparini F, Egidi F, Goings J, Peng B, Petrone A, Henderson T, Ranasinghe D, Zakrzewski V G, Gao J, Rega N, Zheng G, Liang W, Hada M, Ehara M, Toyota K, Fukuda R, Hasegawa J, Ishida M, Nakajima T, Honda Y, Kitao O, Nakai H, Vreven T, Throssell K, Montgomery J A, Jr., Peralta J E, Ogliaro F, Bearpark M, Heyd J J, Brothers E, Kudin K N, Staroverov V N, Keith T, Kobayashi R, Normand J, Raghavachari K, Rendell A, Burant J C, Iyengar S S, Tomasi J, Cossi M, Millam J M, Klene M, Adamo C, Cammi R, Ochterski J W, Martin R L, Morokuma K, Farkas O, Foresman J B. Fox, Gaussian, Inc., Wallingford CT, 2009.
- [8] Tomasi J, Mennucci B, Cammi R. Quantum mechanical continuum solvation models [J]. Chem. Rev., 2005, 105: 2999-3093.
- [9] Lu T, Chen F W. Multiwfn: a multifunctional wavefunction analyzer [J]. J. Comput. Chem., 2012, 33: 580-592.
- [10] Lippert E Z. Dipolmoment and elektronenstruktur von angeregten molekulen. Naturforsch. A, 1955, 10: 541-545.
- [11] Mataga N, Kaifu Y, Koizumi M. The solvent effect on fluorescence spectrum-change of solute-solvent interaction during the lifetime of excited solute molecule [J]. Bull. Chem. Soc. Jpn., 1955, 10: 690-691.